

Greybody Factors for Scalar Fields emitted by a Higher-Dimensional Schwarzschild-de-Sitter Black-Hole

P. Kanti¹, T. Pappas² and N. Pappas³

*Division of Theoretical Physics, Department of Physics,
University of Ioannina, Ioannina GR-45110, Greece*

Abstract

In this work, we consider the propagation of scalar particles in a higher-dimensional Schwarzschild-de-Sitter black-hole spacetime, both on the brane and in the bulk. Our analysis applies for arbitrary partial modes and for both minimal and non-minimal coupling of the scalar field. A general expression for the greybody factor is analytically derived in each case, and its low-energy behaviour is studied in detail. Its profile in terms of scalar properties (angular-momentum number and non-minimal coupling parameter) and spacetime properties (number of extra dimensions and cosmological constant) is thoroughly investigated. In contrast to previous studies, the effect of the cosmological constant is taken into account both close to and far away from the black-hole horizon. The dual role of the cosmological constant, that may act either as a helping agent to the emission of scalar particles or as a deterring effect depending on the value of the non-minimal coupling parameter, is also demonstrated.

¹Email: pkanti@cc.uoi.gr

²Email: thpap@cc.uoi.gr

³Email: npappas@cc.uoi.gr

1 Introduction

After the revival of the theories postulating the existence of extra dimensions at the turn of the previous century [1, 2], the existence and properties of black-hole solutions in the novel geometrical set-up were widely reconsidered in the literature. Especially, the effect of the emission of Hawking radiation [3] – being the manifestation of a quantum effect in a gravitational context – by higher-dimensional black holes attracted particular attention. Different types of black-hole spacetimes were considered and different species of emitted particles were studied. It was soon realised that the Hawking radiation spectra may provide a wealth of information regarding the higher-dimensional gravitational background, such as the number of extra spacelike dimensions [4, 5, 6], the magnitude and orientation of the angular-momentum of the produced black hole [7, 8, 9, 10, 11, 12, 13, 14, 15, 16, 17], the value of higher-derivative gravitational couplings [18] or the effect of the brane [19, 20] (for a more extensive, but still incomplete, list of references, see the reviews [21]-[31]).

In the presence of a cosmological constant, the spacetime around such a black hole takes the form of the higher-dimensional Schwarzschild-de-Sitter or Tangherlini solution [32]. The propagation of a scalar field in the spacetime around this type of black hole was studied both analytically and numerically in [33]. However, the analytical study was limited to the case of the lowest partial mode and in the very low-energy regime, since the presence of the cosmological constant increases the complexity of the field equations and makes the analytic treatment particularly difficult. A later work [34] extended the analysis by computing the next-to-leading-order term in the expansion of the greybody factor in terms of the energy of the scalar particle, focusing again on the lowest partial mode. More recently, an analysis [35] restricted in the 4-dimensional case produced results for the greybody factor for arbitrary scalar partial modes.

The present work aims at filling a gap in the literature concerning the existence of analytical results for the greybody factor for arbitrary modes of a scalar field propagating in the spacetime of a higher-dimensional Schwarzschild-de-Sitter black hole. The cases of scalar fields living both on the brane and in the bulk will be considered, as well as the cases of minimal and non-minimal coupling. An effort will be made to improve the accuracy of our analysis by avoiding approximations in the form of the metric tensor employed in previous works [34, 35] that aimed at simplifying the field equations. An appropriately chosen radial coordinate will allow us to analytically integrate the radial equation and take into account the full effect of the bulk cosmological constant both close to and far away from the black-hole horizon. Analytical expressions for the greybody factor will be derived, and their approximate forms up to terms of $\mathcal{O}(\omega^2)$ for both minimal and non-minimal couplings will be determined. The asymptotic low-energy values of the greybody factor will be found in each case, and the role of the non-minimal coupling parameter will be investigated also in a higher-dimensional context. Finally, the dual role of the cosmological constant will be examined: in the case of minimal coupling, this quantity is known [33] to enhance the value of the greybody factor and to give a boost to the emission of scalar fields both in the bulk and on the brane; in the presence of a non-minimal coupling, the cosmological constant also acts as an effective mass for the scalar field and thus tends to decrease the value of the greybody factor. We will show that the decisive factor for the net effect of the cosmological constant is the value of the

non-minimal coupling parameter.

The outline of our paper is as follows: in Section 2, we present the gravitational background under consideration, both the higher-dimensional one in the bulk and the induced one on the brane. In Section 3, we focus on the propagation of scalar fields on the brane: we solve the radial equation for arbitrary partial modes and value of the non-minimal coupling parameter, study analytically its low-energy limits and examine its profile in terms of both particle and spacetime properties. In Section 4, the whole analysis is performed for a scalar field living in the bulk. We present our conclusions in Section 5.

2 The Gravitational Background

Let us first consider a purely higher-dimensional gravitational theory of the form

$$S_D = \int d^{4+n}x \sqrt{-G} \left(\frac{R_D}{2\kappa_D^2} - \Lambda \right), \quad (1)$$

where $D = 4 + n$ is the total number of dimensions, n an arbitrary number of space-like dimensions, $\kappa_D^2 = 1/M_*^{2+n}$ the higher-dimensional gravitational constant associated with the fundamental scale of gravity M_* , and Λ a positive bulk cosmological constant.

The variation of the above action with respect to the metric tensor G_{MN} leads to the Einstein's field equations

$$R_{MN} - \frac{1}{2} G_{MN} R_D = -\kappa_D^2 G_{MN} \Lambda \equiv \kappa_D^2 T_{MN}, \quad (2)$$

where T_{MN} is the bulk energy-momentum tensor. From the above, by contraction with G^{MN} , we may easily find that the higher-dimensional Ricci scalar R_D is given by the following expression

$$R_D = \frac{2(n+4)}{n+2} \kappa_D^2 \Lambda, \quad (3)$$

in terms of the bulk cosmological constant.

We will assume the existence of a spherically-symmetric $(4+n)$ -dimensional gravitational background of the form

$$ds^2 = -h(r) dt^2 + \frac{dr^2}{h(r)} + r^2 d\Omega_{2+n}^2, \quad (4)$$

where $d\Omega_{2+n}^2$ is the area of the $(2+n)$ -dimensional unit sphere given by

$$d\Omega_{2+n}^2 = d\theta_{n+1}^2 + \sin^2 \theta_{n+1} \left(d\theta_n^2 + \sin^2 \theta_n \left(\dots + \sin^2 \theta_2 (d\theta_1^2 + \sin^2 \theta_1 d\varphi^2) \dots \right) \right), \quad (5)$$

with $0 \leq \varphi < 2\pi$ and $0 \leq \theta_i \leq \pi$, for $i = 1, \dots, n+1$. Then, the field equations (2) lead to the well-known Tangherlini solution [32]

$$h(r) = 1 - \frac{\mu}{r^{n+1}} - \frac{2\kappa_D^2 \Lambda r^2}{(n+3)(n+2)}, \quad (6)$$

describing a higher-dimensional Schwarzschild-de-Sitter spacetime. In the above, the parameter μ is given by [36]

$$\mu = \frac{\kappa_D^2 M}{(n+2)} \frac{\Gamma[(n+3)/2]}{\pi^{(n+3)/2}}, \quad (7)$$

where M is the black-hole mass. The equation $h(r) = 0$ has, in principle, $(n+3)$ roots, however, not all of them are real and positive. Depending on the values of the parameters M and Λ , the Schwarzschild-de-Sitter spacetime, either four or higher-dimensional, may have two, one or zero horizons [37]. In the context of the present analysis, the values of our parameters will be chosen so that the spacetime always has two horizons, the black-hole one r_h and the cosmological one r_c , with the region of interest being the area in between ($r_h < r < r_c$).

According to the brane-world models [1, 2], four-dimensional observers are restricted to live on the brane. Therefore, although the gravitational background is generically higher-dimensional, all phenomenologically interesting effects take place in the projected-on-the-brane spacetime. This follows by fixing the value of the extra angular coordinates, $\theta_i = \pi/2$, for $i = 2, \dots, n+1$, and has the form

$$ds^2 = -h(r) dt^2 + \frac{dr^2}{h(r)} + r^2 (d\theta^2 + \sin^2 \theta d\varphi^2). \quad (8)$$

Note that the metric function $h(r)$ is still given by Eq. (6). The above spacetime is neither a vacuum solution nor a solution describing a 4-dimensional Schwarzschild-de-Sitter spacetime. Instead, it satisfies the projected-on-the-brane Einstein's field equations in the presence of an effective energy-momentum tensor. By explicit calculation, one may find that the curvature of this 4-dimensional background is given by the expression

$$R_4 = \frac{24\kappa_D^2 \Lambda}{(n+2)(n+3)} + \frac{n(n-1)\mu}{r^{n+3}}, \quad (9)$$

and it is clearly generated by a non-trivial brane distribution of matter according to the AdS/CFT correspondence.

In what follows, we will assume that the above higher-dimensional black hole emits scalar particles both in the bulk and on the brane. These particles will carry small quanta of mass or energy compared to the black hole mass so that the gravitational background, both bulk and brane, will remain unchanged.

3 Emission of Scalar Particles on the Brane

We will first focus on the case of the emission of brane-localised scalar particles as the most phenomenologically interesting one. We will consider a general scalar field theory in which the scalar field may couple to gravity either minimally or non-minimally, namely

$$S_4 = \frac{1}{2} \int d^4x \sqrt{-g} [(1 - \xi \Phi^2) R_4 - \partial_\mu \Phi \partial^\mu \Phi]. \quad (10)$$

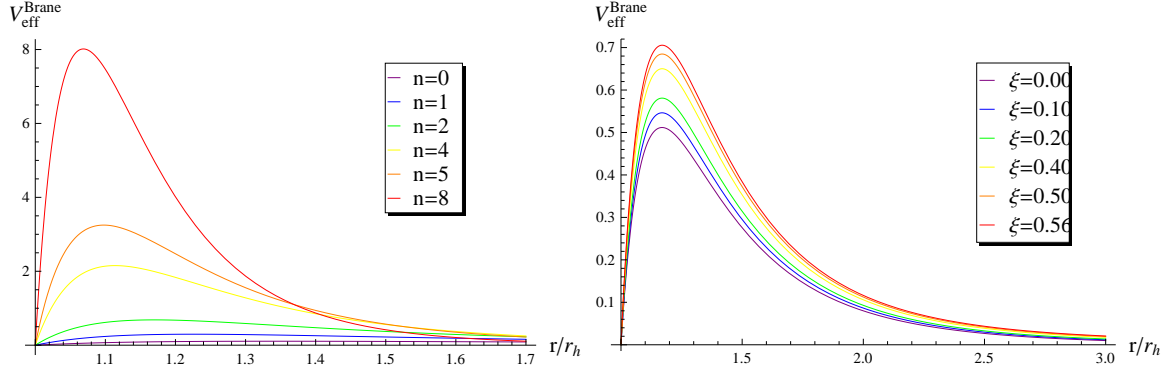


Figure 1: Effective potential for brane scalar fields for: **(a)** $l = 0$, $\Lambda = 0.01 r_h^{-2}$, $\xi = 0.5$ and variable $n = 0, 1, 2, 4, 5, 8$ (from bottom to the top), and **(b)** $l = 0$, $\Lambda = 0.01 r_h^{-2}$, $n = 2$ and variable $\xi = 0, 0.1, 0.2, 0.4, 0.5, 0.56$ (again, from bottom to top).

In the above expression, $g_{\mu\nu}$ is the projected metric tensor on the brane and R_4 the corresponding brane curvature given in Eqs. (8) and (9), respectively. Also, ξ is an arbitrary constant parameter that determines the magnitude of the coupling between the scalar and the gravitational field on the brane with the value $\xi = 0$ corresponding to the minimal coupling.

The equation of motion of the aforementioned scalar field has the form

$$\frac{1}{\sqrt{-g}} \partial_\mu (\sqrt{-g} g^{\mu\nu} \partial_\nu \Phi) = \xi R_4 \Phi. \quad (11)$$

Assuming the factorized ansatz

$$\Phi(t, r, \theta, \varphi) = e^{-i\omega t} R(r) Y(\theta, \varphi), \quad (12)$$

where $Y(\theta, \varphi)$ are the scalar spherical harmonics, and using the well-known eigenvalue equation that these satisfy, we obtain the following decoupled radial equation for the function $R(r)$

$$\frac{1}{r^2} \frac{d}{dr} \left(h r^2 \frac{dR}{dr} \right) + \left[\frac{\omega^2}{h} - \frac{l(l+1)}{r^2} - \xi R_4 \right] R = 0. \quad (13)$$

Before attempting to analytically solve the above equation in order to determine the greybody factor for the emission of brane-localised scalar fields by a higher-dimensional Schwarzschild-de-Sitter black hole, let us first study the profile of the effective potential that characterizes such an emission process. We redefine the radial function as $u(r) = rR(r)$ and use the tortoise coordinate $dr_* = dr/h(r)$; then, Eq. (13) may be re-written in the Schrödinger-like form

$$-\frac{d^2 u(r)}{dr_*^2} + V_{\text{eff}}^{\text{brane}} u(r) = \omega^2 u(r), \quad (14)$$

where the effective potential has the form

$$V_{\text{eff}}^{\text{brane}} = h(r) \left[\frac{l(l+1)}{r^2} + \xi R_4 + \frac{1}{r} \frac{dh}{dr} \right], \quad (15)$$

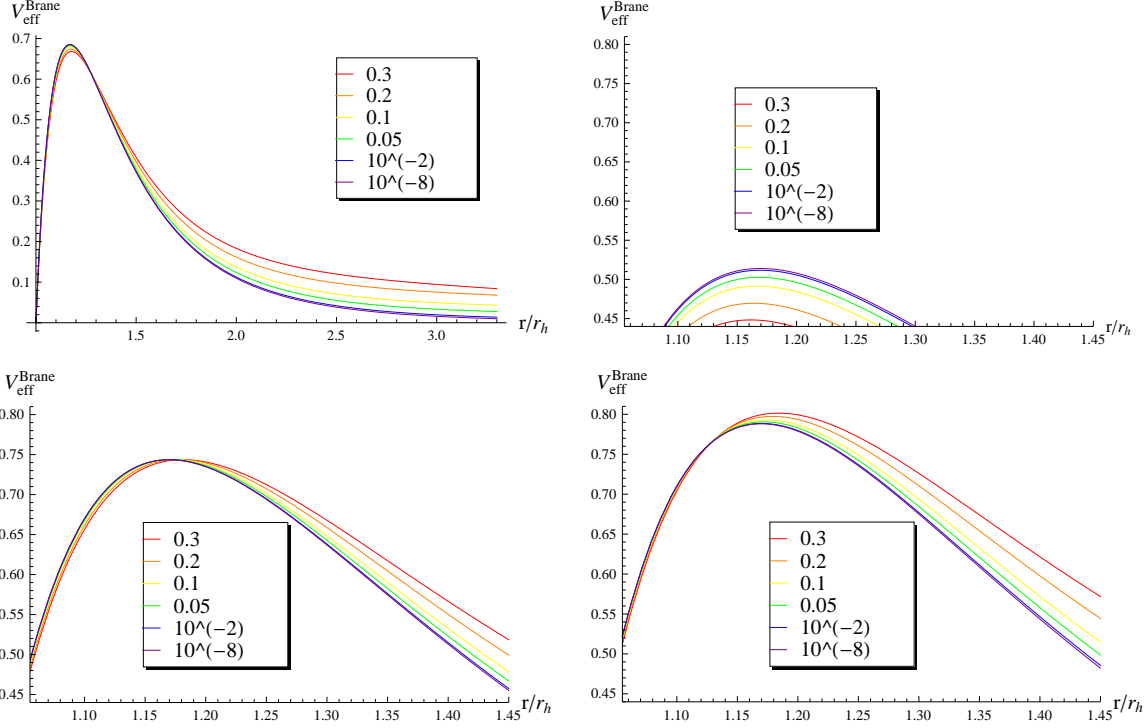


Figure 2: Effective potential for brane scalar fields for $l = 0$, $n = 2$, and variable $\Lambda = 10^{-8}, 10^{-2}, 0.05, 0.1, 0.2, 0.3$ (in units of r_h^{-2}), and **(a)** wide view for $\xi = 0.5$, and magnifications of the peak area for **(b)** $\xi = 0$, **(c)** $\xi = 0.67$ and **(d)** $\xi = 0.8$.

or more explicitly

$$V_{\text{eff}}^{\text{brane}} = h(r) \left\{ \frac{l(l+1)}{r^2} + \frac{4\kappa_D^2 \Lambda (6\xi - 1)}{(n+2)(n+3)} + \frac{\mu}{r^{n+3}} [(n+1) + \xi n(n-1)] \right\}. \quad (16)$$

The effective potential vanishes at the two horizons, r_h and r_c , due to the vanishing of the metric function $h(r)$. The parameter μ can be eliminated by using the equation for the black-hole horizon, i.e.

$$\mu = r_h^{n+1} \left(1 - \frac{2\kappa_D^2 \Lambda r_h^2}{(n+2)(n+3)} \right), \quad (17)$$

and, then, by fixing the value of the black-hole horizon, one can study the profile of the effective potential in terms of the angular-momentum number l , number of extra dimensions n , coupling constant ξ and cosmological constant Λ .

From Eq. (16), it is obvious that the height of the gravitational barrier increases with the angular-momentum number l leading to the well-known suppression of the emission of partial modes with large l ; however, the dependence on the other three parameters of the model is less clear. Therefore, in Fig. 1, we depict the profile of the effective potential in terms of the number of extra dimensions n and coupling constant ξ : the increase in the value of n causes again an increase in the height of the gravitational barrier and

subsequently the suppression of the emission of scalar fields on the brane as it was shown in [33]; a similar effect arises with the increase of ξ which was also noted in the context of a purely 4-dimensional theory [35]. In Fig. 2, we display the dependence of the barrier on the cosmological constant. The dependence here is more subtle, as the magnifications of the peak area, shown in Figs. 2(b,c,d), demonstrate: for a minimally-coupled scalar field, i.e. $\xi = 0$, the barrier decreases with Λ and the emission of scalar particles is thus enhanced, as it was demonstrated in [33]; as the value of the coupling constant increases, the effect of Λ on the height of the barrier is gradually reduced; finally, beyond a critical value of ξ , the situation is reversed with the barrier now increasing with any increase in the value of the cosmological constant.

3.1 The Analytical Solution

The differential equation (13) cannot be analytically solved over the whole radial regime, even in the absence of the non-minimal coupling. Therefore, an approximate method must be applied in which the radial equation is solved at specific radial regimes, i.e. close to the black-hole and cosmological horizons, and then the corresponding solutions are smoothly matched at the low-energy limit. For a Schwarzschild-de-Sitter spacetime, this technique was applied for the lowest partial mode $l = 0$ in the context of a higher-dimensional model [33, 34] for minimally-coupled scalar fields, and more recently for arbitrary l and non-vanishing ξ in the purely 4-dimensional case [35]. We will now address the most general case of a scalar field propagating on the brane background (8) and with or without a non-minimal coupling.

We will start by solving the radial equation in the regime close to the black-hole horizon. Previous studies [34, 35], in order to simplify the analysis, have ignored the presence of the cosmological constant close to the black-hole area and approximated the metric by a purely Schwarzschild one, either four or higher-dimensional. In contrast to this, and in an attempt to make our results as accurate as possible, we will keep all effects of the presence of the cosmological constant to the black-hole physics. But then, finding the appropriate radial coordinate transformation, necessary to bring Eq. (13) to a more familiar form, turns out to be a real challenge. To our knowledge, the most convenient such transformation is the following

$$r \rightarrow f(r) = \frac{h(r)}{1 - \tilde{\Lambda}r^2}, \quad (18)$$

where, for convenience, we have defined $\tilde{\Lambda} \equiv 2\kappa_D^2\Lambda/(n+2)(n+3)$. Also, henceforth, we will set $\kappa_D^2 = 1$. The new variable f may be alternatively written as

$$f(r) = 1 - \frac{\mu}{r^{n+1}} \frac{1}{1 - \tilde{\Lambda}r^2} = 1 - \left(\frac{r_h}{r}\right)^{n+1} \frac{(1 - \tilde{\Lambda}r_h^2)}{(1 - \tilde{\Lambda}r^2)}, \quad (19)$$

and thus ranges from 0, at $r \simeq r_h$, to 1 as $r \gg r_h$. In addition, it satisfies the relation

$$\frac{df}{dr} = \frac{1-f}{r} \frac{A(r)}{1 - \tilde{\Lambda}r^2}, \quad (20)$$

where $A(r) \equiv (n+1) - (n+3)\tilde{\Lambda}r^2$. By using the above, Eq. (13) can be re-written, at $r \simeq r_h$, as:

$$f(1-f) \frac{d^2 R}{df^2} + (1-B_h f) \frac{dR}{df} + \left[\frac{(\omega r_h)^2}{A_h^2 f} - \frac{\lambda_h (1 - \tilde{\Lambda} r_h^2)}{A_h^2 (1-f)} \right] R = 0. \quad (21)$$

In the above, A_h is the value of $A(r)$ evaluated at $r = r_h$, and we have further defined

$$B_h \equiv 1 + \frac{n}{A_h} (1 - \tilde{\Lambda} r_h^2) + \frac{4\tilde{\Lambda} r_h^2}{A_h^2}, \quad \lambda_h = l(l+1) + \xi R_4^{(h)} r_h^2, \quad (22)$$

with $R_4^{(h)}$ the brane curvature (9) evaluated at $r = r_h$.

We now make the following field redefinition: $R(f) = f^{\alpha_1} (1-f)^{\beta_1} F(f)$. Then, Eq. (21) takes the form of a hypergeometric equation,

$$f(1-f) \frac{d^2 F}{df^2} + [c_1 - (1+a_1+b_1)f] \frac{dF}{df} - a_1 b_1 F = 0, \quad (23)$$

under the identifications

$$a_1 = \alpha_1 + \beta_1 + B_h - 1 \quad b_1 = \alpha_1 + \beta_1, \quad c_1 = 1 + 2\alpha_1. \quad (24)$$

We then need to determine the power coefficients α_1 and β_1 ; these are found by solving the following second-order algebraic equations:

$$\alpha_1^2 + \frac{\omega^2 r_h^2}{A_h^2} = 0, \quad (25)$$

and

$$\beta_1^2 + \beta_1 (B_h - 2) + \frac{\omega^2 r_h^2}{A_h^2} - \frac{\lambda_h (1 - \tilde{\Lambda} r_h^2)}{A_h^2} = 0. \quad (26)$$

The corresponding solutions are

$$\alpha_1^{(\pm)} = \pm \frac{i\omega r_h}{A_h}, \quad (27)$$

and

$$\beta_1^{(\pm)} = \frac{1}{2} \left[(2 - B_h) \pm \sqrt{(B_h - 2)^2 + \frac{4\lambda_h (1 - \tilde{\Lambda} r_h^2)}{A_h^2}} \right]. \quad (28)$$

The general solution of the hypergeometric equation (23), combined with the relation between $R(f)$ and $F(f)$, leads to the following expression for the radial function $R(f)$ in the near-black-hole-horizon regime:

$$\begin{aligned} R_{BH}(f) &= A_1 f^{\alpha_1} (1-f)^{\beta_1} F(a_1, b_1, c_1; f) \\ &+ A_2 f^{-\alpha_1} (1-f)^{\beta_1} F(a_1 - c_1 + 1, b_1 - c_1 + 1, 2 - c_1; f), \end{aligned} \quad (29)$$

where $A_{1,2}$ are arbitrary constants. Near the horizon, f goes to zero, and the above reduces to

$$R_{BH}(f) \simeq A_1 f^{\alpha_1} + A_2 f^{-\alpha_1}. \quad (30)$$

The two choices therefore for the parameter α_1 are equivalent, under the simultaneous interchange of the arbitrary coefficients $A_{1,2}$. As we observed earlier, the effective potential vanishes at the black-hole horizon, thus we expect the general solution there to have the form of free plane waves, i.e.

$$R_{BH}(r_*) = \frac{u_{BH}(r_*)}{r_h} = \tilde{A}_1 e^{-i\omega r_*} + \tilde{A}_2 e^{i\omega r_*}. \quad (31)$$

Clearly, for $f \propto e^{A_h r_*/r_h}$, the two expressions match under the proper redefinitions of the integration constants. As a result, the two choices $\alpha_1^{(\pm)}$ simply interchange the incoming and outgoing plane waves at the black-hole horizon. To remove this arbitrariness, we set $\alpha_1 = \alpha_1^{(-)}$. Then, imposing the boundary condition that no outgoing waves are to be found just outside the black-hole horizon, demands setting $A_2 = \tilde{A}_2 = 0$. Finally, the sign in the expression of the β_1 coefficient may be decided from the criterion for the convergence of the hypergeometric function $F(a_1, b_1, c_1; f)$, namely $\mathbf{Re}(c_1 - a_1 - b_1) > 0$, which clearly demands that we choose $\beta_1 = \beta_1^{(-)}$.

We now turn to the radial regime close to the cosmological horizon r_c . Here, we will follow the previous studies [34, 35] and approximate the metric function by

$$h(r) = 1 - \left(\frac{r_h}{r}\right)^{(n+1)} - \tilde{\Lambda} r^2 \left[1 - \left(\frac{r_h}{r}\right)^{(n+3)}\right] \simeq 1 - \tilde{\Lambda} r^2, \quad (32)$$

where we have again used Eq. (17) in order to eliminate the μ parameter. Clearly, the validity of the above approximation increases the farther away we move from the black-hole horizon, i.e. the larger r_c or the smaller Λ is. In addition, the same approximation becomes more accurate the larger the number of extra dimensions is; therefore, we expect that this analytic approach will lead to results with a more extended validity regime compared to the ones derived in the purely 4-dimensional case.

If we then make the change of variable $r \rightarrow h(r) \simeq 1 - \tilde{\Lambda} r^2$, the radial equation (13) in the area close to $r = r_c$ takes the form

$$h(1-h) \frac{d^2 R}{dh^2} + \left(1 - \frac{5}{2}h\right) \frac{dR}{dh} + \frac{1}{4} \left[\frac{(\omega r_c)^2}{h} - \frac{l(l+1)}{(1-h)} - \xi R_4^{(c)} r_c^2 \right] R = 0, \quad (33)$$

where now $R_4^{(c)}$ is the brane curvature (9) evaluated at $r = r_c$. By making the field redefinition: $R(h) = h^{\alpha_2} (1-h)^{\beta_2} X(h)$, Eq. (33) takes again the form of a hypergeometric equation (23) where now the various indices take the form

$$a_2 = \alpha_2 + \beta_2 + \frac{3}{4} + \sqrt{\frac{9}{16} - \frac{\xi R_4^{(c)} r_c^2}{4}}, \quad (34)$$

$$b_2 = \alpha_2 + \beta_2 + \frac{3}{4} - \sqrt{\frac{9}{16} - \frac{\xi R_4^{(c)} r_c^2}{4}}, \quad c_2 = 1 + 2\alpha_2. \quad (35)$$

The power coefficients α_2 and β_2 are in this case determined by the equations

$$\alpha_2^2 + \frac{\omega^2 r_c^2}{4} = 0, \quad (36)$$

and

$$\beta_2^2 + \frac{\beta_2}{2} - \frac{l(l+1)}{4} = 0, \quad (37)$$

respectively, and read

$$\alpha_2^{(\pm)} = \pm \frac{i\omega r_c}{2}, \quad \beta_2^{(\pm)} = \frac{1}{4} \left[-1 \pm (2l+1) \right]. \quad (38)$$

The general solution of the radial equation in the cosmological-horizon regime can then be written as

$$R_C(h) = B_1 h^{\alpha_2} (1-h)^{\beta_2} X(a_2, b_2, c_2; h) + B_2 h^{-\alpha_2} (1-h)^{\beta_2} X(a_2 - c_2 + 1, b_2 - c_2 + 1, 2 - c_2; h), \quad (39)$$

where $B_{1,2}$ are again arbitrary constants. The criterion for the convergence of the hypergeometric function $X(a_2, b_2, c_2; h)$, namely $\mathbf{Re}(c_2 - a_2 - b_2) > 0$, forces us again to choose the negative sign in the expression of the β_2 coefficient that then reads $\beta_2 = -(l+1)/2$.

The metric function $h(r)$ goes again to zero when $r \rightarrow r_c$. Then, the solution very close to the cosmological horizon reduces to the expression

$$R_C(h) \simeq B_1 h^{\alpha_2} + B_2 h^{-\alpha_2}. \quad (40)$$

Since the effective potential vanishes also at r_c , the solution is again expected to be comprised in that area by free plane waves. Indeed, setting $h = e^{-2r_*/r_c}$, the above asymptotic solution may be re-written as

$$R_C(r_*) \simeq B_1 e^{\mp i\omega r_*} + B_2 e^{\pm i\omega r_*}. \quad (41)$$

Once again, the choice of the sign in the expression of α_2 , simply interchanges the incoming and outgoing waves. In contrast to what happens at the black-hole horizon, both waves are now allowed to exist at $r \simeq r_c$, and it is their amplitudes that define the greybody factor for the emission of scalar fields by the back hole. Thus, if we choose $\alpha_2 = \alpha_2^{(+)}$, the greybody factor is simply given by

$$|A|^2 = 1 - \left| \frac{B_2}{B_1} \right|^2. \quad (42)$$

In order to complete the solution, we must ensure that the two asymptotic solutions, R_{BH} and R_C , can be smoothly matched at some arbitrary intermediate value of the radial coordinate. Starting from the near-black-hole solution, Eq. (29) with $A_2 = 0$, we first shift the argument of the hypergeometric function from f to $1-f$, by using the general relation [38]

$$F(a, b, c; x) = \frac{\Gamma(c) \Gamma(c-a-b)}{\Gamma(c-a) \Gamma(c-b)} F(a, b, a+b-c+1; 1-x) + (1-f)^{c-a-b} \frac{\Gamma(c) \Gamma(a+b-c)}{\Gamma(a) \Gamma(b)} F(c-a, c-b, c-a-b+1; 1-x), \quad (43)$$

where x is an arbitrary variable. Then, in the limit $r \gg r_h$, or $f \rightarrow 1$, R_{BH} takes the ‘stretched’ form

$$\begin{aligned} R_{BH}(r) &\simeq A_1 \frac{\Gamma(c_1) \Gamma(a_1 + b_1 - c_1)}{\Gamma(a_1) \Gamma(b_1)} \left(\frac{r}{r_h}\right)^{-(l+1)} + A_1 \frac{\Gamma(c_1) \Gamma(c_1 - a_1 - b_1)}{\Gamma(c_1 - a_1) \Gamma(c_1 - b_1)} \left(\frac{r}{r_h}\right)^l \\ &\equiv \Sigma_1 r^{-(l+1)} + \Sigma_2 r^l. \end{aligned} \quad (44)$$

In the above, we have made the approximation that, for small cosmological constant Λ and coupling constant ξ , we may write

$$(1 - f)^{\beta_1} \simeq \left(\frac{r_h}{r}\right)^{\beta_1(n+1)} \simeq \left(\frac{r}{r_h}\right)^l \quad (45)$$

$$(1 - f)^{\beta_1 + c_1 - a_1 - b_1} \simeq \left(\frac{r_h}{r}\right)^{(2 - B_h - \beta_1)(n+1)} \simeq \left(\frac{r}{r_h}\right)^{-(l+1)}, \quad (46)$$

since in that limit it holds that: $A_h \simeq (n+1)$, $B_h \simeq (2n+1)/(n+1)$ and $\beta_1 \simeq -l/(n+1)$. Note that the aforementioned approximations are applied only in the expressions of the multiplying factors $(1 - f)$ and not in the arguments of the Gamma functions in order to increase the validity of our analytical results.

We now turn to the solution near the cosmological horizon (39). Applying the same general relation (43), in this case for the variable h , we obtain

$$\begin{aligned} R_C(r) &\simeq \left(\frac{r}{r_c}\right)^{-(l+1)} \left[B_1 \frac{\Gamma(c_2) \Gamma(c_2 - a_2 - b_2)}{\Gamma(c_2 - a_2) \Gamma(c_2 - b_2)} + B_2 \frac{\Gamma(2 - c_2) \Gamma(c_2 - a_2 - b_2)}{\Gamma(1 - a_2) \Gamma(1 - b_2)} \right] \\ &+ \left(\frac{r}{r_c}\right)^l \left[B_1 \frac{\Gamma(c_2) \Gamma(a_2 + b_2 - c_2)}{\Gamma(a_2) \Gamma(b_2)} + B_2 \frac{\Gamma(2 - c_2) \Gamma(a_2 + b_2 - c_2)}{\Gamma(a_2 + 1 - c_2) \Gamma(b_2 + 1 - c_2)} \right] \\ &\equiv (\Sigma_3 B_1 + \Sigma_4 B_2) r^{-(l+1)} + (\Sigma_5 B_1 + \Sigma_6 B_2) r^l. \end{aligned} \quad (47)$$

Here, we have made again the approximations

$$(1 - h)^{\beta_2} \simeq \left(\frac{r}{r_c}\right)^{2\beta_2} = \left(\frac{r}{r_c}\right)^{-(l+1)} \quad (48)$$

$$(1 - h)^{\beta_2 + c_2 - a_2 - b_2} \simeq \left(\frac{r}{r_c}\right)^{-(1+2\beta_2)} = \left(\frac{r}{r_c}\right)^l, \quad (49)$$

valid again for small cosmological constant Λ and small coupling constant ξ .

The two ‘stretched’ solutions (44) and (47) have the same power-law form and their smooth matching is straightforward: identifying the coefficients of the same powers of r , we arrive at the constraints

$$B_1 = \frac{\Sigma_1 \Sigma_6 - \Sigma_2 \Sigma_4}{\Sigma_3 \Sigma_6 - \Sigma_4 \Sigma_5}, \quad B_2 = \frac{\Sigma_2 \Sigma_3 - \Sigma_1 \Sigma_5}{\Sigma_3 \Sigma_6 - \Sigma_4 \Sigma_5}. \quad (50)$$

Then, it is easy to write the expression of the greybody factor (42) for the emission of scalar fields by a higher-dimensional Schwarzschild-de-Sitter black hole on the brane; this

has the form

$$|A^2| = 1 - \left| \frac{\Sigma_2 \Sigma_3 - \Sigma_1 \Sigma_5}{\Sigma_1 \Sigma_6 - \Sigma_2 \Sigma_4} \right|^2. \quad (51)$$

A few comments are in order at this point regarding the approximations made in our analysis. The assumed range of values of the variables f and h as well as their approximated forms are indeed highly accurate as long as the value of the cosmological constant is small and the distance between r_h and r_c is large. As soon as Λ becomes large, deviations from the expected behaviour for the greybody factor will start to appear. We will explicitly demonstrate this in section 3.3 and thus define the range of validity of our analytical results. Finally, let us stress that the aforementioned approximations, necessary for the smooth matching of the two asymptotic solutions, do not involve at all the energy of the emitted particle. To our knowledge, this is in contrast with all previous similar studies where a low-energy condition was always imposed. This creates the expectation that our analytic result may be valid beyond the low-energy regime. We will return again to this point in section 3.3.

3.2 The Low-energy Limit

In this subsection, we will derive a simplified expression for the greybody factor (51) in the low-energy limit, i.e. when $\omega \rightarrow 0$, in the case of both minimal and non-minimal coupling. In the former case, we will focus on the dominant partial wave with $l = 0$, and demonstrate that our expression correctly reproduces the non-vanishing asymptotic value derived previously in the literature [33]. In the latter case, we will analytically show that, in the limit $\omega \rightarrow 0$, the aforementioned asymptotic value disappears as does also the $\mathcal{O}(\omega)$ term in the expansion of the greybody factor. The first non-vanishing term of $\mathcal{O}(\omega^2)$ for arbitrary l and coupling parameter ξ will be presented.

We will present a unified analysis for scalars with minimal and non-minimal coupling by keeping the parameter ξ arbitrary, and consider particular values at a later stage. For the low-energy expansion, it is convenient to re-write the (a_i, b_i, c_i) parameters of the hypergeometric functions in a way that separates the ω -dependence. To this end, we define the ω -independent quantities

$$\delta = \frac{1 + 2n - \sqrt{1 + 4\lambda_h}}{2(n + 1)}, \quad (52)$$

$$\epsilon = \frac{1 - \sqrt{1 + 4\lambda_h}}{2(n + 1)}, \quad (53)$$

$$\eta_{\pm} = \frac{1}{4} \left(1 - 2l \pm \sqrt{9 - 4\xi R_4^{(c)} r_c^2} \right), \quad (54)$$

and write

$$a_1 = \delta - \frac{i\omega r_h}{(n + 1)}, \quad b_1 = \epsilon - \frac{i\omega r_h}{(n + 1)}, \quad c_1 = 1 - \frac{2i\omega r_h}{(n + 1)}, \quad (55)$$

for the parameters near the black-hole horizon, and

$$a_2 = \eta_+ + \frac{i\omega r_c}{2}, \quad b_2 = \eta_- + \frac{i\omega r_c}{2}, \quad c_2 = 1 + i\omega r_c, \quad (56)$$

for the ones close to the cosmological horizon. Note that above, in order to simplify the fairly complex calculation, we have also taken the limit of small cosmological constant apart from the terms where ξ is involved.

Then, the Σ_i quantities, defined in Eqs. (44) and (47), can be written in the form

$$\Sigma_1 = \frac{r_h^{l+1} \Gamma(1 - 2i\omega R_H) \Gamma(\delta + \epsilon - 1)}{\Gamma(\delta - i\omega R_H) \Gamma(\epsilon - i\omega R_H)}, \quad (57)$$

$$\Sigma_2 = \frac{r_h^{-l} \Gamma(1 - 2i\omega R_H) \Gamma(1 - \delta - \epsilon)}{\Gamma(1 - \delta - i\omega R_H) \Gamma(1 - \epsilon - i\omega R_H)}, \quad (58)$$

$$\Sigma_3 = \frac{r_c^{(l+1)} \Gamma(1 + 2i\omega R_C) \Gamma(1 - \eta_+ - \eta_-)}{\Gamma(1 - \eta_+ + i\omega R_C) \Gamma(1 - \eta_- + i\omega R_C)}, \quad (59)$$

$$\Sigma_4 = \frac{r_c^{(l+1)} \Gamma(1 - 2i\omega R_C) \Gamma(1 - \eta_+ - \eta_-)}{\Gamma(1 - \eta_+ - i\omega R_C) \Gamma(1 - \eta_- - i\omega R_C)} = \overline{\Sigma_3}, \quad (60)$$

$$\Sigma_5 = \frac{r_c^{-l} \Gamma(1 + 2i\omega R_C) \Gamma(\eta_+ + \eta_- - 1)}{\Gamma(\eta_+ + i\omega R_C) \Gamma(\eta_- + i\omega R_C)}, \quad (61)$$

$$\Sigma_6 = \frac{r_c^{-l} \Gamma(1 - 2i\omega R_C) \Gamma(\eta_+ + \eta_- - 1)}{\Gamma(\eta_+ - i\omega R_C) \Gamma(\eta_- - i\omega R_C)} = \overline{\Sigma_5}, \quad (62)$$

where we have also defined $R_H \equiv r_h/(n+1)$ and $R_C \equiv r_c/2$.

We first consider the minimal coupling case, and focus on the lowest, dominant mode of the scalar field. Upon setting $\xi = 0$ and $l = 0$, the quantities in Eqs. (52)-(54) are greatly simplified and read

$$\delta = \frac{n}{n+1}, \quad \epsilon = 0, \quad \eta_{\pm} = \left(1, -\frac{1}{2}\right). \quad (63)$$

Then, the Σ_i quantities also assume simpler forms that may easily be expanded in power series in the energy ω . For example, Σ_1 is written as

$$\Sigma_1 \approx \frac{r_h \Gamma(1 - \frac{2i\omega r_h}{n+1}) \Gamma(-\frac{1}{n+1})}{\Gamma(\frac{n-i\omega r_h}{n+1}) \Gamma(-\frac{i\omega r_h}{n+1})} \rightarrow i\omega r_h^2 + \mathcal{O}(\omega^2). \quad (64)$$

In the above, we have applied the Gamma function property: $z \Gamma[-z] = -\Gamma[1-z]$, and used the expansion formulae [38]

$$\Gamma(\hat{a} + i\omega \hat{b}) = \Gamma(\hat{a}) \left[1 + i\omega \hat{b} \Psi^{(0)}(\hat{a})\right] + \mathcal{O}(\omega^2), \quad (65)$$

$$\Gamma(i\omega \hat{b}) = \frac{1}{i\omega \hat{b}} - \gamma + \mathcal{O}(\omega), \quad (66)$$

where \hat{a} and \hat{b} are arbitrary ω -independent quantities, γ is the Euler's constant, and $\Psi^{(0)}$ the poly-gamma function. Similar expressions follow for the other Σ_i quantities, namely

$$\Sigma_2 \approx 1 + \frac{i\omega r_h}{n+1} \left[\gamma + \Psi^{(0)}\left(\frac{1}{n+1}\right) \right] + \mathcal{O}(\omega^2), \quad (67)$$

$$\Sigma_3 \approx i\omega r_c^2 + \mathcal{O}(\omega^2) = \overline{\Sigma}_4, \quad (68)$$

$$\Sigma_5 \approx 1 + i\omega r_c (\log 2 - 1) + \mathcal{O}(\omega^2) = \overline{\Sigma}_6. \quad (69)$$

Under these approximations we finally obtain, from Eq. (51), the result

$$|A^2| = 1 - \left| \frac{i\omega (r_c^2 - r_h^2)}{i\omega (r_c^2 + r_h^2)} \right|^2 + \mathcal{O}(\omega) = \frac{4r_h^2 r_c^2}{(r_c^2 + r_h^2)^2} + \mathcal{O}(\omega). \quad (70)$$

Therefore, our general expression (51) correctly reproduces the low-energy geometric value of the greybody factor for the mode $l = 0$, in accordance to previous analyses [33, 34, 35]. This feature is characteristic of the propagation of free, massless scalar particles in a Schwarzschild-de-Sitter spacetime, both four- and higher-dimensional, and leads to the enhanced emission of very soft modes in the Hawking radiation spectra [33].

Let us now assume that the non-minimal coupling parameter ξ takes an arbitrary non-vanishing value. In this case, we observe that all Σ_i quantities are proportional to the following combination:

$$\frac{\Gamma(1 \pm 2i\omega R)}{\Gamma(\hat{a} \pm i\omega R) \Gamma(\hat{b} \pm i\omega R)} = \frac{1 \mp i\omega R \left[2\gamma + \Psi^{(0)}(\hat{a}) + \Psi^{(0)}(\hat{b}) \right]}{\Gamma(\hat{a}) \Gamma(\hat{b})} + \mathcal{O}(\omega^2), \quad (71)$$

where R is either R_H or R_C , \hat{a} and \hat{b} are again arbitrary, but non-vanishing, ω -independent quantities. Then, using the above expansion formula, we find that

$$\begin{aligned} \Sigma_1 \Sigma_5 &= K (1 - i\omega R_C B + i\omega R_H \Gamma), \\ \Sigma_1 \Sigma_6 &= K (1 + i\omega R_C B + i\omega R_H \Gamma), \\ \Sigma_2 \Sigma_3 &= E (1 + i\omega R_H Z - i\omega R_C \Theta), \\ \Sigma_2 \Sigma_4 &= E (1 + i\omega R_H Z + i\omega R_C \Theta), \end{aligned} \quad (72)$$

where

$$\begin{aligned} K &\equiv \frac{r_h^{(l+1)} r_c^{-l} \Gamma(\delta + \epsilon - 1) \Gamma(\eta_+ + \eta_- - 1)}{\Gamma(\delta) \Gamma(\epsilon) \Gamma(\eta_+) \Gamma(\eta_-)}, \\ E &\equiv \frac{r_h^{-l} r_c^{l+1} \Gamma(1 - \delta - \epsilon) \Gamma(1 - \eta_+ - \eta_-)}{\Gamma(1 - \delta) \Gamma(1 - \epsilon) \Gamma(1 - \eta_+) \Gamma(1 - \eta_-)}, \end{aligned} \quad (73)$$

and

$$\begin{aligned} B &\equiv 2\gamma + \Psi^{(0)}(\eta_+) + \Psi^{(0)}(\eta_-), \\ \Gamma &\equiv 2\gamma + \Psi^{(0)}(\delta) + \Psi^{(0)}(\epsilon) \\ Z &\equiv 2\gamma + \Psi^{(0)}(1 - \delta) + \Psi^{(0)}(1 - \epsilon), \\ \Theta &\equiv 2\gamma + \Psi^{(0)}(1 - \eta_+) + \Psi^{(0)}(1 - \eta_-). \end{aligned} \quad (74)$$

Then, we easily find

$$\begin{aligned} \Sigma_2 \Sigma_3 - \Sigma_1 \Sigma_5 &= (E - K) + i\omega R_H (EZ - K\Gamma) + i\omega R_C (KB - E\Theta), \\ \Sigma_1 \Sigma_6 - \Sigma_2 \Sigma_4 &= (K - E) + i\omega R_H (K\Gamma - EZ) + i\omega R_C (KB - E\Theta), \end{aligned} \quad (75)$$

from which it follows that

$$|\Sigma_2\Sigma_3 - \Sigma_1\Sigma_5|^2 \simeq |\Sigma_1\Sigma_6 - \Sigma_2\Sigma_4|^2 = (K - E)^2 + \mathcal{O}(\omega^2). \quad (76)$$

Substituting the above result in Eq. (51), we find that the first non-vanishing term in the low-energy expansion of the greybody factor, in the case where $\xi \neq 0$, is the one of $\mathcal{O}(\omega^2)$. This holds for all partial waves including the dominant one with $l = 0$. Therefore, in the presence of a non-minimal coupling to gravity, there are no scalar modes with a non-vanishing low-energy asymptotic value of their greybody factor.

The exact expression of the $\mathcal{O}(\omega^2)$ term for arbitrary l is extremely difficult to derive analytically. Therefore, we merely display here its expression derived via symbolic calculation; it has the form

$$|A|^2 = \frac{8\pi^2(\omega r_h)^2 \lambda_h^l [\Gamma(\theta_+) \Gamma(\theta_-)]^2 \Gamma[\frac{1+u}{2(n+1)}] \Gamma[\frac{1+2n+u}{2(n+1)}]}{(1+2l)u \left(\cos[\frac{n\pi}{(n+1)}] + \cos[\frac{\pi u}{(n+1)}] \right) \Gamma[\frac{1}{2} + l]^2 \Gamma[\frac{u}{(n+1)}]^2 \Gamma[\frac{1+2n-u}{2(n+1)}] \Gamma[\frac{1-u}{2(n+1)}]} \quad (77)$$

where $u \equiv \sqrt{(2l+1)^2 + 4\xi R_4^{(h)} r_h^2}$, and

$$\theta_{\pm} = \frac{1}{4} \left(3 + 2l \pm \sqrt{9 - 4\xi R_4^{(c)} r_c^2} \right). \quad (78)$$

As an additional consistency check, we have confirmed that the above expression reduces⁴, after setting $n = 0$, to the one derived in [35] in the context of the four-dimensional analysis.

3.3 Plotting our analytic result

We are now ready to investigate in detail the complete form of the greybody factor for the emission of scalar fields on the brane by a higher-dimensional Schwarzschild-de-Sitter black hole, as this is given by the analytic expression (51). We will also study its dependence on both particle (l, ξ) and spacetime properties (n, Λ).

In Fig. 3, we depict the greybody factor $|A|^2$ as a function of the dimensionless energy parameter ωr_h . The graph on the left, Fig. 3(a), shows the behaviour of $|A|^2$ for the first five partial waves with $l = 0, 1, 2, 3, 4$, for $n = 2$ and $\Lambda = 0.1$ (in units of r_h^{-2}); for every value of the angular-momentum number l , the solid line corresponds to the case of minimal coupling, with $\xi = 0$, and the dashed line to an arbitrary non-minimal coupling, with $\xi = 0.3$. As expected from the dependence of the effective potential on l , the greybody factor gets suppressed for large l , thus rendering the lowest partial wave with $l = 0$ the dominant one; this holds independently of whether the scalar field is coupled minimally or non-minimally to gravity. The presence of ξ causes a significant modification to the behaviour of $|A|^2$ only for the $l = 0$ partial wave: in accordance to the discussion in the previous subsection, for $\xi = 0$ we recover the non-vanishing low-energy geometric value of the greybody factor (70), whereas for $\xi \neq 0$ this limit becomes zero.

⁴The agreement is almost perfect since our result differs by the one appearing in [35] by only a factor 4^l caused perhaps by a typographical error.

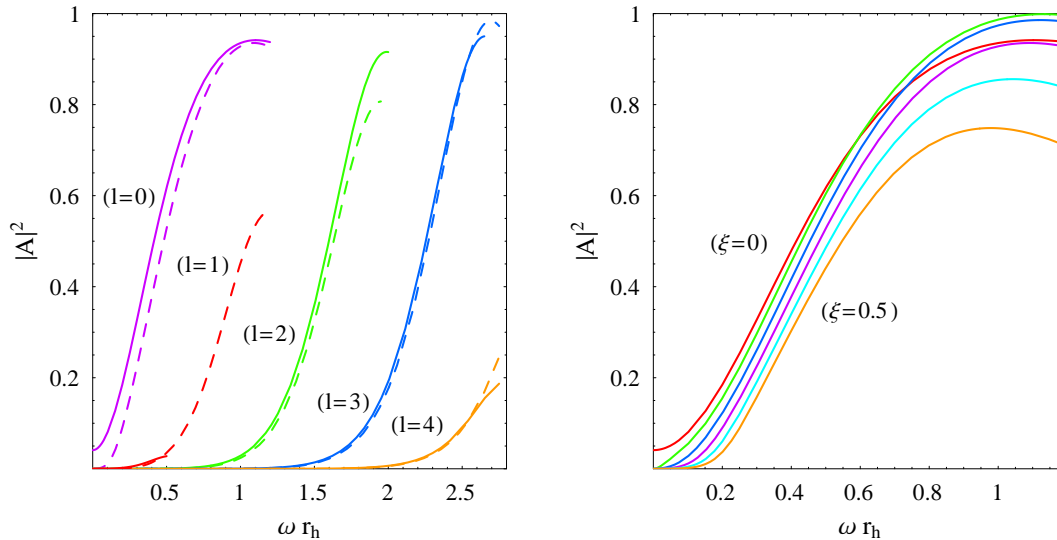


Figure 3: Greybody factors for brane scalar fields, for $n = 2$ and $\Lambda = 0.1$, and: **(a)** for variable $l = 0, 1, 2, 3, 4$ and $\xi = 0$ (solid lines) or $\xi = 0.3$ (dashed lines); **(b)** for $l = 0$ and variable $\xi = 0, 0.1, 0.2, 0.3, 0.4, 0.5$.

We note that, in order to be able to display the behaviour of all five partial waves in the same plot, we were forced to extend the energy range well beyond the low-energy regime, where $\omega r_h \ll 1$. For most partial waves shown, almost the whole of the curve of the greybody factor, extending in principle from zero to unity, is also visible. This is rather unusual in results following from an analytical approach, and, as we commented at the end of Section 3.1, this may be due to the fact that the energy parameter was never involved in the approximations made. As the low-energy assumption is always the reason that the analytic results deviate from the exact numerical ones as the energy increases, we envisage that in the present case our results may be fairly close to the exact ones even for large values of energy. We should however add that our analytic results still show occasional signs of defects caused by the existence of poles in the expression of Gamma functions – this is an inherent feature of the analytic approach used in general in studying Hawking radiation in black-hole spacetimes which employs hypergeometric functions. It is the existence of such a pole that causes the abrupt stop of the solid line for the partial wave with $l = 1$ in Fig. 3(a) at a fairly small value of energy. Although the presence of the non-minimal coupling parameter ξ apparently affects only marginally the behaviour of $|A|^2$ for the case $l \neq 0$, its presence shifts the value of the energy where the pole emerges: it is for this reason that the dashed curve for the partial wave with $l = 1$ manages to extend up to the intermediate energy regime.

In Fig. 3(b), we display the dependence of the greybody factor on the other particle parameter, its coupling parameter ξ : for the lowest partial wave with $l = 0$, $n = 2$ and $\Lambda = 0.1$, $|A|^2$ is plotted for $\xi = 0, 0.1, 0.2, 0.3, 0.4, 0.5$. The transition from the non-zero low-energy asymptotic value to a zero one, as ξ assumes a non-vanishing value, is again evident. We also observe that the greybody factor is suppressed as the value of the coupling parameter increases, again in accordance with the behaviour of the effective

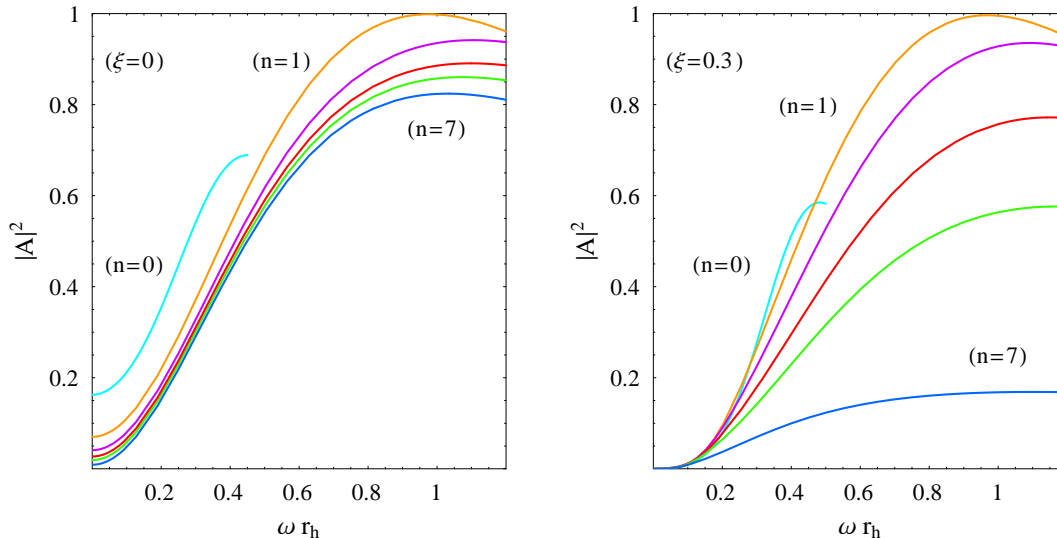


Figure 4: Greybody factors for brane scalar fields, for $l = 0$, $\Lambda = 0.1$, and variable $n = 0, 1, 2, 3, 4, 7$ and: **(a)** for $\xi = 0$, and **(b)** $\xi = 0.3$.

potential. This suppression is similar to the one caused by the presence of a mass term for the scalar field that has been found before in the literature in different black-hole spacetimes [39, 40, 41, 42] – indeed, the way the non-minimal coupling term appears in the scalar equation of motion (11) resembles the one of a mass term. Also, in the purely four-dimensional analysis of [35], it was proposed that this resemblance between the two terms is the one that causes the vanishing of the low-energy asymptotic value of the greybody factor when $\xi \neq 0$: the geometric asymptotic value (70) is characteristic of a free, massless particle, as shown in [33], while a massive scalar particle does not exhibit such a feature. The same behaviour noted in [35] is also observed in the present higher-dimensional set-up, a result that adds further support to this argument.

Next, we turn to the dependence of the greybody factor on the spacetime parameters. In Fig. 4(a,b), we show the behaviour of $|A|^2$ in terms of the number of extra dimensions n , for minimal ($\xi = 0$) and non-minimal ($\xi = 0.3$) coupling, respectively – the remaining parameters have been set to $l = 0$ and $\Lambda = 0.1$. Although the scalar field is not free to propagate in the bulk, the projected spacetime on the brane (8) depends on n , and this is reflected in the profile of the greybody factor. For $\xi = 0$, and in the low-energy limit, $|A|^2$ goes to its geometric value (70), as expected. Although this expression does not have either an explicit dependence on n , it has an implicit one since the location of r_h and r_c , the roots of the metric function $h(r)$ (6), depends on n . Fig. 4(a) shows that, the asymptotic geometric value decreases, as n increases from 0 to 7; this is due to the fact that, for fixed Λ , the increase in the value of n causes the two horizons to move farther apart – this increases the size of the causal spacetime that the scalar field needs to traverse and decreases the corresponding greybody factor. The decrease with n characterizes the behaviour of $|A|^2$ over the whole energy regime, and the same effect persists also for non-zero ξ , as one may see in Fig. 4(b). In fact, the suppression here is much more prominent, especially for large values of n .

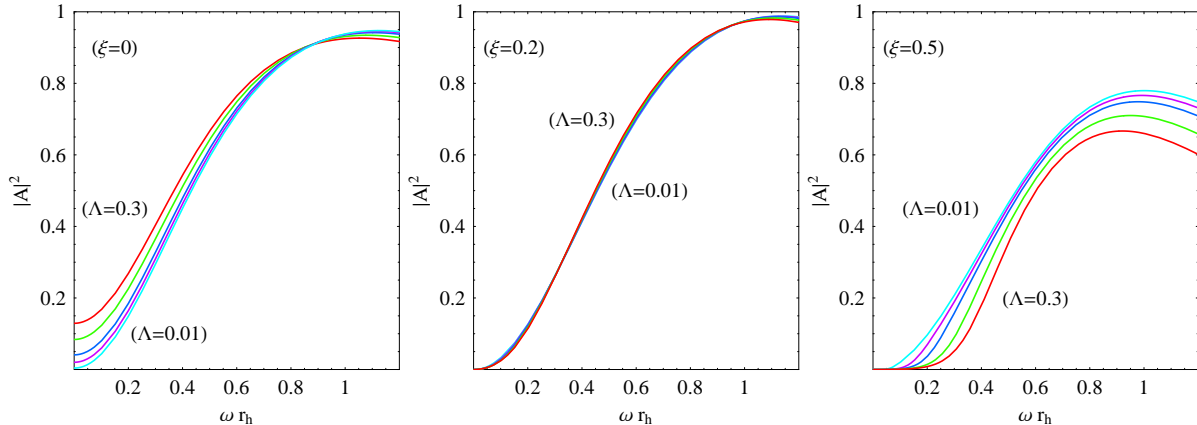


Figure 5: Greybody factors for brane scalar fields for $l = 0$, $n = 2$, and $\Lambda = 0.01, 0.05, 0.1, 0.2, 0.3$, and **(a)** for $\xi = 0$, **(b)** $\xi = 0.2$, and **(c)** $\xi = 0.5$.

Finally, in Fig. 5, we depict the dependence of the greybody factor on the bulk cosmological constant, for three different values of the non-minimal coupling parameter, $\xi = 0, 0.2$ and 0.5 , for the dominant partial wave with $l = 0$ and for $n = 2$. For $\xi = 0$, the value of $|A|^2$ is clearly enhanced as Λ gradually takes on the values $0.01, 0.05, 0.1, 0.2$ and 0.3 - the enhancement seems to disappear beyond the intermediate energy regime but the validity of our analytic approach may also be in question there. As ξ increases, the value of the greybody factor becomes less sensitive to the value of Λ , and eventually, for $\xi = 0.2$ (as shown in Fig. 5(b)), $|A|^2$ is almost independent of it. For even higher values of the coupling parameter, the situation is reversed: now, the greybody factor is suppressed as Λ increases (see Fig. 5(c)). This behaviour is the result of the competition between two different Λ -contributions: one in the metric function, that works towards subsidizing the energy of the emitted particle thus giving a boost to its greybody factor [33], and one in the non-minimal coupling term that, acting as a mass term, suppresses its emission probability. For zero or very small values of ξ , the latter effect is negligible and the former dominates; for intermediate values, the two effects cancel each other, while for large values of ξ , the latter effect is the most important.

As shown in Fig. 5(a), for the case of minimal coupling, i.e. for $\xi = 0$, the greybody factor of the dominant $l = 0$ partial wave adopts a low-energy non-zero asymptotic value. Provided that the approximations considered in our analysis are respected, this asymptotic value should be given by the one in Eq. (70) - this value has been confirmed by exact numerical analyses both in a higher-dimensional [33] and four-dimensional context [35]. However, for large values of the cosmological constant, i.e. larger than $\Lambda = 0.3$, the low-energy asymptotic value of $|A|^2$, as given by the expression (51), deviates from the exact one (70) by more than 10% while for $\Lambda \leq 0.1$ the error falls below 4%. This is due to the fact that, as Λ increases, some of our approximations, such as (32), are not satisfied anymore. Demanding that the deviation between the derived and expected asymptotic limits is smaller than 5% sets the allowed range of values of the cosmological constant that may be considered to $\Lambda \leq 0.1$. It is worth noting that, even when Λ takes a large value, increasing the value of n restores the accuracy of the analysis; this is, for

example, obvious from Eq. (32) where the terms that need to be ignored become indeed more negligible the larger n is.

4 Emission of Scalar Particles in the Bulk

We will now consider the case of the emission of scalar particles in the bulk that may be again minimally or non-minimally coupled to gravity. Then, the higher-dimensional action (1) is supplemented by the scalar part

$$S_\Phi = -\frac{1}{2} \int d^{4+n}x \sqrt{-G} [\xi \Phi^2 R_D + \partial_M \Phi \partial^M \Phi] . \quad (79)$$

where now G_{MN} is the higher-dimensional metric tensor defined in Eq. (4), and R_D the corresponding curvature given in Eq. (3).

The equation of motion of the bulk scalar field now reads

$$\frac{1}{\sqrt{-G}} \partial_M \left(\sqrt{-G} G^{MN} \partial_N \Phi \right) = \xi R_D \Phi . \quad (80)$$

We assume the factorized ansatz

$$\Phi(t, r, \theta_i, \varphi) = e^{-i\omega t} R(r) \tilde{Y}(\theta_i, \varphi) , \quad (81)$$

where $\tilde{Y}(\theta_i, \varphi)$ are the hyperspherical harmonics [43]. Their equation is the $(n+2)$ -dimensional generalisation of the usual two-dimensional one for the scalar harmonics, with eigenvalue $l(l+n+1)$. The angular and radial part are again decoupled with the equation for the radial function $R(r)$ given by

$$\frac{1}{r^{n+2}} \frac{d}{dr} \left(h r^{n+2} \frac{dR}{dr} \right) + \left[\frac{\omega^2}{h} - \frac{l(l+n+1)}{r^2} - \xi R_D \right] R = 0 . \quad (82)$$

If we redefine the radial function as $u(r) = r^{(n+2)/2} R(r)$ and use again the tortoise coordinate $dr_* = dr/h(r)$, then, Eq. (82) may be re-written in the Schrödinger-like form where now the effective potential reads

$$V_{\text{eff}}^{\text{bulk}} = h(r) \left[\frac{l(l+n+1)}{r^2} + \xi R_D + \frac{(n+2)}{2r} \frac{dh}{dr} + \frac{n(n+2)h}{4r^2} \right] , \quad (83)$$

or more explicitly

$$V_{\text{eff}}^{\text{bulk}} = h(r) \left\{ \frac{(2l+n+1)^2 - 1}{4r^2} + \kappa_D^2 \Lambda (n+4) \left[\frac{2\xi}{(n+2)} - \frac{1}{2(n+3)} \right] + \frac{(n+2)^2 \mu}{4r^{n+3}} \right\} . \quad (84)$$

The parameter μ can again be eliminated by using Eq. (17) and the black-hole horizon fixed at an arbitrary value. As is obvious from the above, the bulk effective potential vanishes at the two horizons, r_h and r_c , and its height increases again with the angular-momentum number l . Its profile in terms of the number of extra dimensions n and

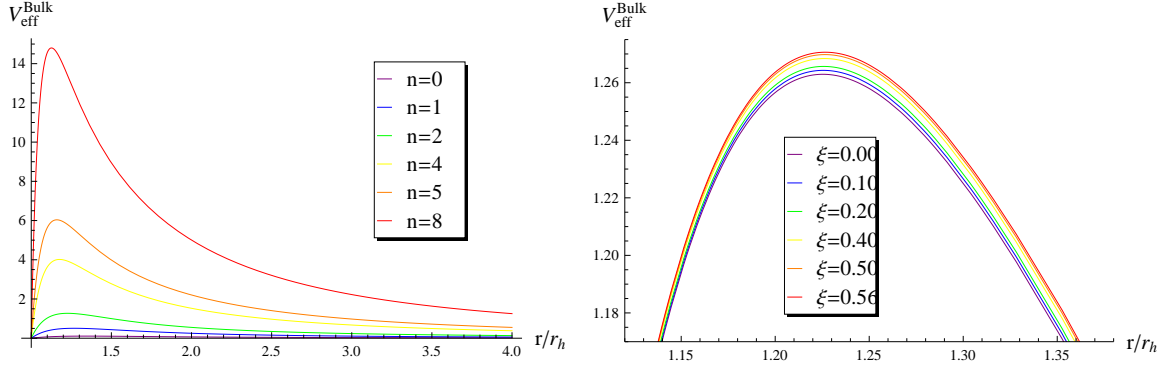


Figure 6: Effective potential for bulk scalar fields for: **(a)** $l = 0$, $\Lambda = 0.01$, $\xi = 0.5$ and variable $n = 0, 1, 2, 4, 5, 8$ (from bottom to the top), and **(b)** $l = 0$, $\Lambda = 0.01$, $n = 2$ and variable $\xi = 0, 0.1, 0.2, 0.4, 0.5, 0.56$ (again, from bottom to top).

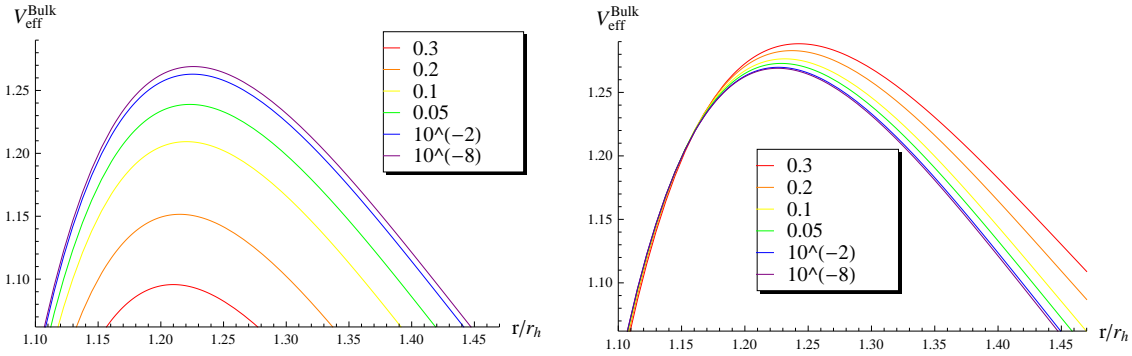


Figure 7: Effective potential for bulk scalar fields for $l = 0$, $n = 2$, and variable $\Lambda = 10^{-8}, 10^{-2}, 0.05, 0.1, 0.2, 0.3$: magnifications of the peak area for **(a)** $\xi = 0$, and **(b)** $\xi = 0.5$.

coupling parameter ξ is shown in Figs. 6(a,b), respectively. As in the case of propagation on the brane, the gravitational barrier in the bulk also rises as either n or ξ increases. We note that the height of the barrier in the bulk is higher than the one on the brane which points to the dominance of brane emission over the bulk one, as noted also before for the case of minimal coupling [33]. Also, the bulk potential is much less sensitive to the value of the non-minimal coupling parameter, and this is why a magnification of the area around the peak of the potential is shown in Fig. 6(b).

The dependence of the bulk potential on the cosmological constant Λ is similar to the one on the brane. Figures 7(a,b) depict the profile of the gravitational barrier for various values of Λ and for minimal, $\xi = 0$, and an arbitrary non-minimal coupling, $\xi = 0.5$, respectively. Again, we find that for zero or small values of the coupling parameter the height of the barrier decreases with the value of the cosmological constant while beyond a critical value it starts to increase.

4.1 The Analytical Solution

In order to solve analytically the scalar equation of motion in the bulk, we follow the same approximation technique as in section 3.1. Near the black-hole horizon, we make the same change of variable $r \rightarrow f$, given in Eq. (18), in terms of which the radial equation (82), at $r \simeq r_h$, becomes

$$f(1-f) \frac{d^2 R}{df^2} + (1-B_h f) \frac{dR}{df} + \left[\frac{(\omega r_h)^2}{A_h^2} + \frac{(\omega r_h)^2}{A_h^2 f} - \frac{\lambda_h(1-\tilde{\Lambda} r_h^2)}{A_h^2(1-f)} \right] R = 0. \quad (85)$$

In the above, $A_h = (n+1) - (n+3)\tilde{\Lambda} r_h^2$ as before, whereas now

$$B_h \equiv 1 + \frac{4\tilde{\Lambda} r_h^2}{A_h^2}, \quad \lambda_h = l(l+n+1) + \xi R_D r_h^2. \quad (86)$$

Making the field redefinition $R(f) = f^{\alpha_1}(1-f)^{\beta_1} F(f)$, brings the above again into the form (23) of a hypergeometric equation. The expressions of the (a, b, c) parameters are now given by

$$\begin{aligned} a_1 &= \alpha_1 + \beta_1 + \frac{1}{2} \left(B_h - 1 + \sqrt{(B_h - 1)^2 - 4\omega^2 r_h^2 / A_h^2} \right), \\ b_1 &= \alpha_1 + \beta_1 + \frac{1}{2} \left(B_h - 1 - \sqrt{(B_h - 1)^2 - 4\omega^2 r_h^2 / A_h^2} \right), \\ c_1 &= 1 + 2\alpha_1. \end{aligned} \quad (87)$$

Using similar arguments as in Section 3, the power coefficients α_1 and β_1 adopt exactly the same functional forms, i.e.

$$\alpha_1 = -\frac{i\omega r_h}{A_h}, \quad (88)$$

and

$$\beta_1 = \frac{1}{2} \left[(2 - B_h) - \sqrt{(B_h - 2)^2 + \frac{4\lambda_h(1 - \tilde{\Lambda} r_h^2)}{A_h^2}} \right]. \quad (89)$$

with the only difference being the different forms of B_h and λ_h . The general solution of the radial equation (85) in the bulk, in the near-black-hole-horizon regime, again takes the form:

$$R_{BH}(f) = A_1 f^{\alpha_1} (1-f)^{\beta_1} F(a_1, b_1, c_1; f) \quad (90)$$

Near the cosmological horizon r_c , the radial equation (82), in terms of the new variable $h(r) \simeq 1 - \tilde{\Lambda} r^2$, can be written as

$$\begin{aligned} h(1-h) \frac{d^2 R}{dh^2} + \left[1 - \frac{(n+5)}{2} h \right] \frac{dR}{dh} \\ + \frac{1}{4} \left[\frac{(\omega r_c)^2}{h} - \frac{l(l+n+1)}{(1-h)} - \xi(n+4)(n+3) \right] R = 0. \end{aligned} \quad (91)$$

The field redefinition $R(h) = h^{\alpha_2}(1-h)^{\beta_2}X(h)$ brings the above equation in the form of a hypergeometric equation with indices

$$a_2 = \alpha_2 + \beta_2 + \frac{n+3}{4} + \frac{1}{4} \sqrt{(n+3)^2 - 4\xi(n+4)(n+3)}, \quad (92)$$

$$b_2 = \alpha_2 + \beta_2 + \frac{n+3}{4} - \frac{1}{4} \sqrt{(n+3)^2 - 4\xi(n+4)(n+3)}, \quad c_2 = 1 + 2\alpha_2. \quad (93)$$

The power coefficients α_2 and β_2 have now the form

$$\alpha_2 = \frac{i\omega r_c}{2}, \quad \beta_2 = -\frac{(l+n+1)}{2}, \quad (94)$$

and the general solution of the radial equation near the cosmological-horizon is given again by Eq. (39).

The analysis after this point follows closely the one on the brane. The two asymptotic solutions are shifted, then stretched and finally matched at a intermediate radial regime. The identification of the multiplying coefficients in front of the same powers of r , leads to the expressions of the integration constants B_1 and B_2 , and finally to the one of the greybody factor that has again the form of Eq. (51).

4.2 The Low-energy Limit

Similarly to the case of brane emission, we will now attempt to derive a simplified expression for the greybody factor (51) in the bulk in the low-energy limit, and study its asymptotic value both for minimal and non-minimal coupling of the scalar field. The sets of (a_i, b_i, c_i) bulk parameters near the black-hole and cosmological horizons, in the limit of low energy, assume again the forms (55) and (56), respectively, where now the ω -independent quantities are defined as

$$\delta = \frac{1}{2} \left[B_h - \sqrt{(B_h - 2)^2 + \frac{4\lambda_h}{A_h^2}} \right], \quad (95)$$

$$\epsilon = \frac{1}{2} \left[2 - B_h - \sqrt{(B_h - 2)^2 + \frac{4\lambda_h}{A_h^2}} \right], \quad (96)$$

$$\eta_{\pm} = \frac{1}{4} \left[1 - 2l - n \pm \sqrt{(n+3)^2 - 4\xi R_D r_c^2} \right]. \quad (97)$$

In the above, we have also taken the limit of small cosmological constant in order to simplify further the analysis⁵. The Σ_i bulk quantities are also identical to their brane analogues with the only difference being that the exponent $l+1$ of r_h and r_c in the Σ_1 , Σ_3 and Σ_4 quantities is replaced by $l+n+1$.

⁵In this limit, the quantity B_h tends to unity – however, the limit of $B_h \rightarrow 1$ will be taken after the $\omega \rightarrow 0$ limit of the Gamma functions in order to keep the two expansions distinct.

In the case of minimal coupling, and for the lowest, dominant mode of the scalar field, the aforementioned ω -independent quantities are simplified to

$$\delta = B_h - 1, \quad \epsilon = 0, \quad \eta_{\pm} = \left[1, -\frac{(n+1)}{2} \right]. \quad (98)$$

Then, applying the low-energy limit, the Σ_1 quantity is simplified to

$$\Sigma_1 \approx \frac{r_h^{n+1} \Gamma(1 - 2i\omega R_H) \Gamma(B_h - 2)}{\Gamma(B_h - 1) \Gamma(-i\omega R_H)} \rightarrow \frac{i\omega r_h^{n+2}}{(n+1)} + \mathcal{O}(\omega^2). \quad (99)$$

Similarly, we obtain for the remaining Σ_i quantities:

$$\Sigma_2 \approx \Sigma_5 \approx \Sigma_6 \approx 1 + \mathcal{O}(\omega), \quad (100)$$

$$\Sigma_3 \approx \frac{i\omega r_c^{n+2}}{(n+1)} + \mathcal{O}(\omega^2) \approx -\Sigma_4, \quad (101)$$

Under these approximations we finally obtain, from Eq. (51), the result

$$|A^2| = 1 - \left| \frac{i\omega (r_c^{n+2} - r_h^{n+2})}{i\omega (r_c^{n+2} + r_h^{n+2})} \right|^2 + \mathcal{O}(\omega) = \frac{4(r_h r_c)^{(n+2)}}{(r_c^{n+2} + r_h^{n+2})^2} + \mathcal{O}(\omega). \quad (102)$$

Again, our general expression (51), applied in the bulk, correctly reproduces the low-energy geometric value of the greybody factor for the mode $l = 0$, in accordance to previous higher-dimensional analyses [33, 34]. Thus, in the case of minimal coupling, scalar particles with very low energy have a non-vanishing probability of being emitted by a higher-dimensional Schwarzschild-de-Sitter spacetime, also in the bulk. However, due to the presence of the number of extra dimensions n in the exponents of r_h and r_c in the above expression, the magnitude of the low-energy asymptotic value in the bulk is significantly smaller compared to the one on the brane.

Turning to the case of non-minimal coupling, we recall that our argument of the vanishing of the greybody factor up to $\mathcal{O}(\omega)$ on the brane did not use the explicit forms of the $(\delta, \epsilon, \eta_{\pm})$ parameters. Since the functional forms of the Σ_i quantities in the bulk are identical to the ones they assumed on the brane, the same argument holds in the case of bulk emission, too; according to this, all partial waves, including the dominant one with $l = 0$, do not assume non-vanishing low-energy asymptotic values if ξ is different from zero.

The first non-vanishing term in the low-energy expansion of the greybody factor, in the case where $\xi \neq 0$, is therefore of $\mathcal{O}(\omega^2)$. This has the explicit form

$$|A|^2 = \frac{16\pi^8 (r_h/r_c)^{l+n/2} (\omega r_h)^2 \sec^4(w\pi/2) [\Gamma(\theta_+) \Gamma(\theta_-)]^{-2}}{\sigma \sqrt{\sigma^2 + 4\xi R_D r_h^2} \left(\cos\left[\frac{\pi\sigma}{2}\right] + \cos\left[\frac{\pi\sqrt{(n+3)^2 - 4\xi R_D r_c^2}}{2}\right] \right)^2 \Gamma\left[\frac{\sigma}{2}\right]^2 \Gamma[w]^2 \Gamma\left[\frac{1-w}{2}\right]^4} \quad (103)$$

where $\sigma \equiv 2l + n + 1$,

$$w = \frac{\sqrt{(2l + n + 1)^2 + 4\xi R_D r_h^2}}{n + 1} \quad (104)$$

and

$$\theta_{\pm} = \frac{1}{4} \left(1 - 2l - n \pm \sqrt{(n+3)^2 - 4\xi R_D r_c^2} \right). \quad (105)$$

The above reduces again to the 4-dimensional result derived in [35] after setting $n = 0$.

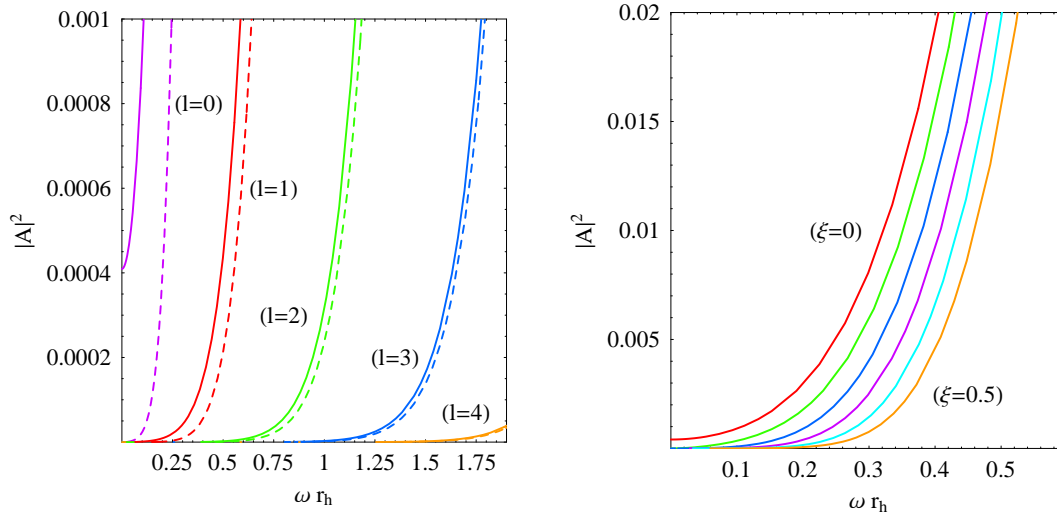


Figure 8: Greybody factors for bulk scalar fields, for $n = 2$ and $\Lambda = 0.1$, and: **(a)** for variable $l = 0, 1, 2, 3$ and $\xi = 0$ (solid lines) or $\xi = 0.3$ (dashed lines); **(b)** for $l = 0$ and variable $\xi = 0, 0.1, 0.2, 0.3, 0.4, 0.5$.

4.3 Plotting our analytic result

We will now study the dependence of the complete form of the greybody factor for bulk scalar fields on both particle properties and spacetime properties. In Fig. 8(a), the greybody factor $|A|^2$ for the first five partial waves with $l = 0, 1, 2, 3, 4$, for $n = 2$ and $\Lambda = 0.1$ (again in units of r_h^{-2}) is depicted; the suppression of the greybody factor as the angular-momentum number l increases is evident. The dashed lines show again the same partial waves but for a non-vanishing value of the non-minimal coupling parameter ξ : a suppression is again observed which becomes less obvious as the angular-momentum number increases. In Fig. 8(b), we focus again on the dominant partial wave ($l = 0$) and study in more detail the dependence of the greybody factor on ξ : here, the suppression is significant and the transition from the non-zero asymptotic value to a vanishing one in the low-energy limit is again easily noticeable.

As it was noted in Section 4.1, the dependence of the effective potential for bulk scalars on the non-minimal coupling parameter ξ is much milder compared to the case of brane scalars. In accordance to this, the modification of the greybody factor as the value of ξ changes is rather limited, and this makes the use of zoom-in plots, like Figs. 8(a,b), necessary. In addition, the presence of n in the expression of the low-energy asymptotic limit of $|A^2|$ for bulk emission (102) suppresses the latter significantly, therefore the magnification of the low-energy regime is necessary in order to observe the transition from the non-vanishing to the vanishing value of the greybody factor of the lowest partial wave as the coupling parameter ξ is turned on.

The value of the greybody factor is suppressed also with the number of extra spacelike dimensions, as shown in Fig. 9. The case of the lowest partial wave is again considered,

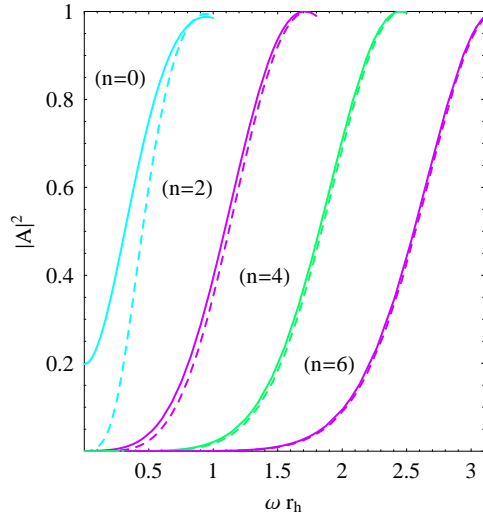


Figure 9: Greybody factors for bulk scalar fields, for $l = 0$, $\Lambda = 0.1$ and variable $n = 0, 2, 4, 6$ and for $\xi = 0$ (solid lines) and $\xi = 0.3$ (dashed lines).

and the dependence on n is shown both for minimal (solid lines) and non-minimal (dashed lines) coupling. It is clear that the suppression with ξ is more significant for the smallest values of the parameter n . Note, that due to poles appearing in the expressions of the Gamma functions, that are present in the form of the greybody factor, no curves for odd values of n were possible to obtain.

In Figs. 10(a,b), we finally depict the dependence of the greybody factor on the bulk cosmological constant, for two values of the non-minimal coupling parameter, $\xi = 0$ and

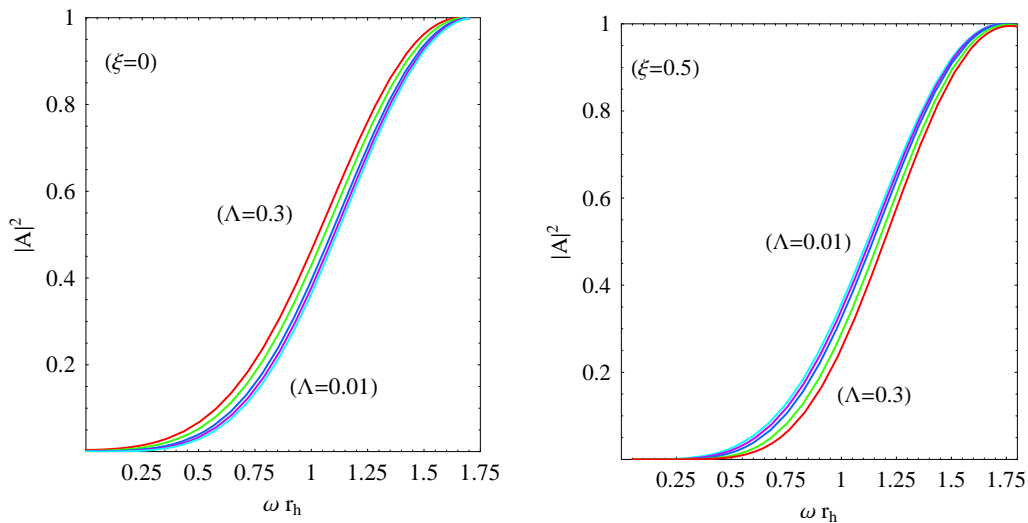


Figure 10: Greybody factors for bulk scalar fields for $l = 0$, $n = 2$, and $\Lambda = 0.01, 0.05, 0.1, 0.2, 0.3$, and **(a)** for $\xi = 0$, and **(b)** $\xi = 0.5$.

0.5, and for the dominant partial wave with $l = 0$. In accordance to the behaviour of the effective potential, we find that the value of $|A^2|$ is indeed enhanced with the bulk cosmological constant provided that the value of ξ is small; beyond a certain value of the coupling parameter, the situation is reversed, and the presence of Λ hinders the emission of scalar fields in the bulk.

5 Conclusions

In the context of the investigation of the Hawking radiation spectra emitted by four- and higher-dimensional black holes, the greybody factors of various species of fields for propagation in these spacetimes have been intensively studied. For the case of a Schwarzschild-de-Sitter black holes, the presence of the cosmological constant increased the complexity of the field equations and made the analytic treatment particularly difficult. Until recently, the existing analytic studies covered the case of only the lowest partial mode of a scalar field in the low-energy approximation [33, 34]. The latest study [35] extended this analysis to the case of arbitrary partial mode but in the strictly four-dimensional case.

In this work, we considered the emission of scalar particles by a higher-dimensional Schwarzschild-de-Sitter black hole both on the brane and in the bulk. Our analysis applied for arbitrary partial modes and, in principle, is valid only at the low-energy regime; however, especially in the case of brane emission where the matching of the solutions did not impose a constraint on the energy of the emitted particle, we envisage that our results may hold well beyond the low-energy regime. In addition, a particular effort was made to take into account the effect of the bulk cosmological constant both close and far away from the black-hole horizon. Near the black-hole horizon particularly, no simplification of the metric tensor was adopted – in contrast to previous studies – and an appropriately chosen new radial coordinate was employed that allowed us to analytically integrate the scalar radial equation in an exact Schwarzschild-de-Sitter spacetime.

Starting from the more phenomenologically interesting case of the emission of scalar fields on the brane, we first derived the analytic form of the greybody factor by following the matching technique of the two asymptotic solutions in the black-hole and cosmological horizons. This expression was first studied analytically, with its low-energy limit computed both for the cases of minimal and non-minimal couplings. In the first case, it was demonstrated that our general expression, for the dominant lowest mode, indeed reduced to the non-vanishing low-energy asymptotic limit found in previous works. We analytically showed that in the presence of a non-minimal coupling of the scalar field with the induced-on-the-brane Ricci scalar, this asymptotic limit vanishes both at $\mathcal{O}(\omega^0)$ and $\mathcal{O}(\omega)$; the analytic expression of the first non-vanishing term at $\mathcal{O}(\omega^2)$ was computed and presented. Then, we studied the profile of the complete result for the greybody factor in terms of particle and spacetime properties. Our results showed that the greybody factor, and thus the emission of scalar particles on the brane by a Schwarzschild-de-Sitter black hole, is suppressed as either the angular-momentum number or the non-minimal coupling parameter increases. The same suppression is observed with the number of extra spacelike dimensions that exist transverse to the brane. In terms of the bulk cosmological constant, we finally demonstrated that its presence acts in two contradictory ways: as a

homogeneously distributed energy over the whole spacetime, it subsidizes the energy of the emitted particle and increases its greybody factor; but, as an effective mass term for the scalar field through the non-minimal coupling term, it decreases its greybody factor – the net effect depends crucially on the value of the non-minimal coupling parameter.

The emission of scalar fields in the bulk by the higher-dimensional Schwarzschild-de-Sitter spacetime was studied next. The corresponding analysis led again to a general expression for the greybody factor valid for arbitrary partial modes and values of the non-minimal coupling parameter with the latter defining the coupling of the bulk scalar field to the curvature of the complete higher-dimensional spacetime. For the case of minimal coupling, the low-energy asymptotic value for the lowest partial mode was again computed and shown to agree with previous studies. A similar analysis for the case of non-minimal coupling, to the one presented for the brane emission, was also performed. The dependence of its complete expression on the various parameters of the theory was also studied in detail and found to follow the same pattern as in the case of brane emission, the main characteristic being the milder dependence of the greybody factor on the non-minimal coupling parameter.

Our results are in excellent agreement with previous analytic results in higher-dimensional [33] and four-dimensional [35] contexts and also follow closely the exact results produced by numerical analysis in the same works. Although, for the case of minimal coupling, the study of the corresponding Hawking radiation spectra by a higher-dimensional Schwarzschild-de-Sitter black hole has been performed [33], the one for a non-minimal coupling, in the same higher-dimensional context, is still lacking. As we believe that the dual role of the cosmological constant in that case may significantly affect the radiation spectra and, perhaps, the bulk-to-brane ratio of emitted energy, we hope to soon report results from such an analysis [44].

Acknowledgements. This research has been co-financed by the European Union (European Social Fund - ESF) and Greek national funds through the Operational Program “Education and Lifelong Learning” of the National Strategic Reference Framework (NSRF) - Research Funding Program: “ARISTEIA. Investing in the society of knowledge through the European Social Fund”. Part of this work was supported by the COST Actions MP0905 “Black Holes in a Violent Universe” and MP1210 “The String Theory Universe”.

References

- [1] N. Arkani-Hamed, S. Dimopoulos and G. R. Dvali, *Phys. Lett. B* **429**, 263 (1998); *Phys. Rev. D* **59**, 086004 (1999); I. Antoniadis, N. Arkani-Hamed, S. Dimopoulos and G. R. Dvali, *Phys. Lett. B* **436**, 257 (1998).
- [2] L. Randall and R. Sundrum, *Phys. Rev. Lett.* **83** (1999) 3370; *Phys. Rev. Lett.* **83** (1999) 4690.
- [3] S. W. Hawking, *Commun. Math. Phys.* **43**, 199–220 (1975)

- [4] P. Kanti and J. March-Russell, Phys. Rev. D **66**, 024023 (2002); Phys. Rev. D **67**, 104019 (2003).
- [5] C. M. Harris and P. Kanti, JHEP **0310**, 014 (2003).
- [6] A. S. Cornell, W. Naylor and M. Sasaki, JHEP **0602**, 012 (2006);
V. Cardoso, M. Cavaglia and L. Gualtieri, Phys. Rev. Lett. **96**, 071301 (2006); JHEP **0602**, 021 (2006);
S. Creek, O. Efthimiou, P. Kanti and K. Tamvakis, Phys. Lett. B **635**, 39 (2006).
- [7] C. M. Harris and P. Kanti, Phys. Lett. B **633** (2006) 106;
G. Duffy, C. Harris, P. Kanti and E. Winstanley, JHEP **0509**, 049 (2005).
- [8] M. Casals, P. Kanti and E. Winstanley, JHEP **0602**, 051 (2006).
- [9] M. Casals, S. Dolan, P. Kanti and E. Winstanley, JHEP **0703**, 019 (2007); JHEP **0806**, 071 (2008).
- [10] D. Ida, K. y. Oda and S. C. Park, Phys. Rev. D **67**, 064025 (2003) [Erratum-ibid. D **69**, 049901 (2004)]; Phys. Rev. D **71**, 124039 (2005); Phys. Rev. D **73**, 124022 (2006).
- [11] S. Creek, O. Efthimiou, P. Kanti and K. Tamvakis, Phys. Rev. D **75** (2007) 084043;
Phys. Rev. D **76** (2007) 104013; Phys. Lett. B **656**, 102 (2007).
- [12] V. P. Frolov and D. Stojkovic, Phys. Rev. D **67**, 084004 (2003);
H. Nomura, S. Yoshida, M. Tanabe and K. i. Maeda, Prog. Theor. Phys. **114**, 707 (2005);
E. Jung and D. K. Park, Nucl. Phys. B **731**, 171 (2005); Mod. Phys. Lett. A **22**, 1635 (2007);
S. Chen, B. Wang, R. K. Su and W. Y. Hwang, JHEP **0803**, 019 (2008).
- [13] H. Kodama, Prog. Theor. Phys. Suppl. **172**, 11 (2008); Lect. Notes Phys. **769**, 427 (2009);
J. Doukas, H. T. Cho, A. S. Cornell and W. Naylor, Phys. Rev. D **80** (2009) 045021;
P. Kanti, H. Kodama, R. A. Konoplya, N. Pappas and A. Zhidenko, Phys. Rev. D **80** (2009) 084016.
- [14] A. Flachi, M. Sasaki and T. Tanaka, JHEP **0905** (2009) 031.
- [15] M. Casals, S. R. Dolan, P. Kanti and E. Winstanley, Phys. Lett. B **680** (2009) 365.
- [16] D. C. Dai and D. Stojkovic, JHEP **1008** (2010) 016.
- [17] M. O. P. Sampaio, JHEP **1203** (2012) 066.
- [18] J. Grain, A. Barrau and P. Kanti, Phys. Rev. D **72** (2005) 104016.
- [19] V. P. Frolov and D. Stojkovic, Phys. Rev. D **66**, 084002 (2002); Phys. Rev. Lett. **89**, 151302 (2002);
D. Stojkovic, Phys. Rev. Lett. **94**, 011603 (2005).

- [20] D. C. Dai, N. Kaloper, G. D. Starkman and D. Stojkovic, Phys. Rev. D **75**, 024043 (2007);
T. Kobayashi, M. Nozawa, Y. Takamizu, Phys. Rev. D **77**, 044022 (2008).
- [21] P. Kanti, Int. J. Mod. Phys. A **19**, 4899–4951 (2004).
- [22] G. L. Landsberg, Eur. Phys. J. C **33**, S927–S931 (2004).
- [23] A. S. Majumdar and N. Mukherjee, Int. J. Mod. Phys. D **14**, 1095–1129 (2005).
- [24] S. C. Park, Prog. Part. Nucl. Phys. **67**, 617–650 (2012).
- [25] B. Webber, eConf C **0507252**, T030 (2005) [hep-ph/0511128].
- [26] A. Casanova and E. Spallucci, Class. Quant. Grav. **23**, R45–R62 (2006).
- [27] P. Kanti, Lect. Notes Phys. **769**, 387–423 (2009).
- [28] P. Kanti, Rom. J. Phys. **57**, 879–893 (2012).
- [29] E. Winstanley, arXiv:0708.2656 [hep-th] (2007).
- [30] P. Kanti, J. Phys. Conf. Ser. **189**, 012020 (2009).
- [31] P. Kanti and E. Winstanley, arXiv:1402.3952 [hep-th].
- [32] F. Tangherlini, Nuovo Cim. **27** (1963) 636.
- [33] P. Kanti, J. Grain and A. Barrau, Phys. Rev. D **71** (2005) 104002.
- [34] T. Harmark, J. Natario and R. Schiappa, Adv. Theor. Math. Phys. **14** (2010) 727.
- [35] L. C. B. Crispino, A. Higuchi, E. S. Oliveira and J. V. Rocha, Phys. Rev. D **87** (2013) 10, 104034.
- [36] R. C. Myers and M. J. Perry, Annals Phys. **172**, 304 (1986).
- [37] C. Molina, Phys. Rev. D **68** (2003) 064007.
- [38] M. Abramowitz and I. Stegun, *Handbook of Mathematical Functions* (Academic, New York, 1996).
- [39] D. N. Page, Phys. Rev. D **16** (1977) 2402.
- [40] E. I. Jung, S. H. Kim and D. K. Park, Phys. Lett. B **586** (2004) 390; JHEP **0409** (2004) 005; Phys. Lett. B **602** (2004) 105.
- [41] M. O. P. Sampaio, JHEP **0910** (2009) 008; JHEP **1002** (2010) 042.
- [42] P. Kanti and N. Pappas, Phys. Rev. D **82** (2010) 024039.
- [43] C. Muller, in *Lecture Notes in Mathematics: Spherical Harmonics* (Springer-Verlag, Berlin-Heidelberg, 1966).
- [44] P. Kanti, T. Pappas and N. Pappas, in progress.